The Structure of the $\left[\mathrm{Zn_{In}}\text{-}\mathrm{V_P}\right]^{Q}$ defect complex in Zn doped InP.

C.W.M. Castleton, S.Mirbt

Theory of Condensed Matter, Department of Physics, Uppsala University,
Box 530, 751 21 Uppsala, Sweden.

Abstract. We study the structure of the $\mathrm{Zn_{In}}$-$\mathrm{V_P}$ defect complex in Zn doped InP as a function of the charge Q on the complex, using plane wave *ab initio* DFT-LDA calculations. We find that for all charge states from at least +2 to -3 the Zn is in a DX like position, sp^2 bonded to three P atoms, with an empty p^z orbital directed across the vacancy towards the triangle of In atoms. Electrons added/removed go to/from localised orbitals centred upon the In triangle, which shortens the In-In distances as (bonding) electrons are added. The Zn-In distances also shorten for electrostatic reasons, so that the vacancy volume is reduced by adding electrons to the complex, as seen in recent experiments.

1. Introduction

Zn doped p-type InP is one of the most common materials in use within optoelectronics. The Zn sits substitutionally within the In sublattice, ($\mathrm{Zn_{In}}$,) where it has a shallow acceptor level. However, a well known limitation in the use of Zn as a p-dopant in InP is the saturation of the hole concentration in the mid 10^{18} cm^{-3} range. Above this further increases in Zn concentration do not translate into increases in hole concentration. There are several suspected causes for this, particularly increases in the concentration of interstitial Zinc, ($\mathrm{Zn_i}$,) phase separation, and the formation of compensative defects, such as phosphorus vacancies ($\mathrm{V_P}$,) and complexes of zinc with $\mathrm{V_P}$. [1]

The formation of one such Zn-$\mathrm{V_P}$ complex has recently been reported by Slotte et al. [2] in samples which have been post-growth annealed in the temperature range 300-600 K. Using positron annihilation they find that the complex has at least two forms, thought to be different charge states of the same complex. One is most stable at room temperature, and has an effective vacancy volume rather larger than that of a free $\mathrm{V_P}$. When the measurement temperature is raised they find that the complex undergoes a transition to a second form, which has a smaller vacancy volume, similar to that of the free vacancy. In this paper we report preliminary results from a study of the $\mathrm{Zn_{In}}$-$\mathrm{V_P}$ complex which we propose to be that observed in the positron annihilation experiments. We will here present a study of the geometry and vacancy volume of the complex, and how that geometry and volume are altered by changes in the charge state of the complex. Details of energetics and more specific comparisons to the experimental results will be published later.

2. Calculational Details.

We use plane wave *ab initio* Density Functional Theory (DFT) within the Local Density Approximation (LDA) together with ultra soft pseudopotentials. Calculations are performed

Table 1. Comparison of k-point convergence of the electronic and structural contributions to ε_{form} . Convergence of the electronic contributions is estimated by $\Delta^{UnRel}\,(\text{2x-4x}) = \varepsilon_{form}^{Unrel}\,(\text{2x2x2}) - \varepsilon_{form}^{Unrel}\,(\text{4x4x4})$ and $\Delta^{UnRel}\,(\text{4x-6x}) = \varepsilon_{form}^{Unrel}\,(\text{4x4x4}) - \varepsilon_{form}^{Unrel}\,(\text{6x6x6})$ whilst the convergence of the structural contributions is estimated as $\Delta^{Rel}\,(\text{2x-4x}) = \varepsilon_{form}^{Rel}\,(\text{2x2x2}) - \varepsilon_{form}^{Rel}\,(\text{4x4x4})$.

Defect	Δ^{UnRel}		Δ^{Rel}	Defect	Δ^{UnRel}		Δ^{Rel}
	(2x-4x)	(4x-6x)	(2x-4x)		(2x-4x)	(4x-6x)	(2x-4x)
V_{In}^{-4}	0.0082		-0.0190	Zn_P^{+2}	-0.0266		0.0095
V_{In}^{0}	-0.0483	0.0093	0.0368	Zn_i^{+2}	0.0117	0.0001	0.0040
In_i^{0}	0.0252	0.0052		Si_{In}^{0}	0.0091		0.0091
In_i^{+1}	-0.0539		-0.0037	Si_{In}^{+1}	0.0048		-0.0038
In_i^{+3}	0.0206	0.0058		Si_{In}^{+2}	0.0891		0.0046
In_i^{+4}	-0.1038		0.0061	Si_P^{-2}	0.0296		-0.0006
P_{In}^{+1}	-0.0360		0.0246	Si_P^{-1}	0.0031		0.0008
P_{In}^{+2}	0.0314		0.0259	Si_P^{0}	0.0734		-0.0027
V_P^{-2}	-0.0607	-0.0123		Si_P^{+1}	0.0279		0.0004
V_P^{+2}	0.0840	0.0012		$\left[Zn_i\text{-}V_P\right]^{+3}$	0.0272		0.0151
Zn_{In}^{+1}	0.0375		0.0007	$\left[Zn_{In}\text{-}V_P\right]^{-1}$	-0.0750		0.0046
Zn_{In}^{0}	0.0807	-0.0011	-0.0025	$\left[Zn_{In}\text{-}V_P\right]^{0}$	0.0057		-0.0029
Zn_{In}^{-1}	-0.0004	0.0000	-0.0005	$\left[Zn_{In}\text{-}V_P\right]^{+1}$	-0.0598		0.0184

using the VASP code. Before doing calculations involving defects we first optimise the lattice constant subject to LDA, finding a value of 5.827 Å, compared to 5.869 Å experimentally. We find a band gap of 0.667 eV compared to 1.344 eV in experiment, and a heat of formation of 0.431 eV compared to 0.728 eV.

For defect calculations we use a 64 atom simple cubic supercell, and allow all atoms not located on the surface of the cell to relax. This restriction is included to truncate the spurious elastic interactions between adjacent supercells. In calculating total energies of supercells containing charged defects we also include a uniform neutralising background charge. The key quantity is the formation energy of the defect, ε_{form} , defined as

$$\varepsilon_{form} = E^T\left(\text{defect}^Q\right) - E^T\left(\text{bulk}\right) + \sum_i \mu_i n_i + Q\left(e_v + e_f\right) \tag{1}$$

where $E^T\left(\text{defect}^Q\right)$ and $E^T\left(\text{bulk}\right)$ are the total energy of the InP supercell with and without the charge Q defect. Both are calculated with the same values of planewave cutoff, k-point grid, etc, in order to make use of cancellation of errors. The defect is formed by adding/removing n_i atoms, each with chemical potential μ_i, and by adding $(-Q)$ electrons, whose chemical potential is the Fermi level e_f, measured from the valence band edge e_v. In the current work we consider only one particular defect, so we can ignore the $\sum_i \mu_i n_i$ term. We then adjust the various calculational parameters to converge ε_{form} . We find that it is

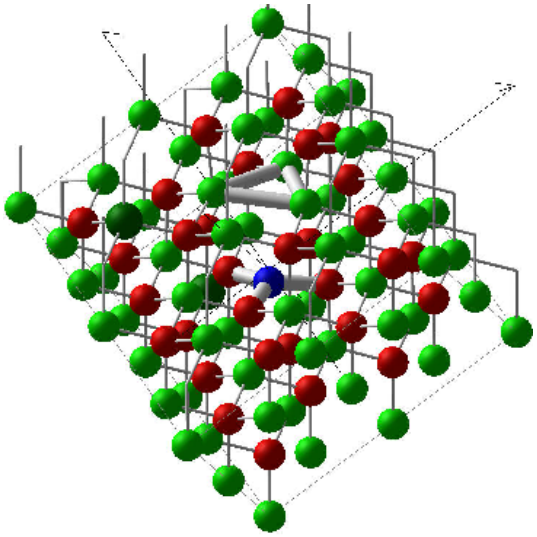

Figure 1. Structure of the 64 atom cubic cell containing the $\left[\mathrm{Zn_{In}\text{-}V_P}\right]^0$ complex. Atom types are green: In, red: P, blue: Zn.

sufficient to use pseudopotentials in which Zn d-electrons are treated as valence electrons but In d-electrons are left in the core. We find that a plane wave cutoff energy of 200eV is enough to converge ε_{form} to $O(0.01\mathrm{eV})$. Real space projection operators are used, with the cutoff chosen to give errors below $O(0.01\mathrm{eV})$. The k point convergence is more interesting. We find that when atomic relaxations are ignored, a 2x2x2 point Monkhorst-Pack grid produces errors below $O(0.01\mathrm{eV})$, provided $Q=0$. When $Q\neq 0$, however, we find that a 4x4x4 grid is required, and the error introduced by truncating at 2x2x2 increases with $\mid Q \mid$. We have tested this across a wide variety of different point defects in InP. (See table 1.) On the other hand, we find that the relaxation energy converges faster. We can define the relaxation energy ε_{Relax} as

$$\varepsilon_{Relax}(\text{k-grid}) = \varepsilon^{Rel}_{form}(\text{k-grid}) - \varepsilon^{Unrel}_{form}(\text{k-grid}) \tag{2}$$

where ε^{Rel}_{form} and $\varepsilon^{Unrel}_{form}$ are ε_{form} including and excluding atomic relaxations. We find that ε_{Relax} is converged for a 2x2x2 Monkhorst-Pack grid, for any value of Q. (Table 1.) In other words the structural contribution to ε_{form} appears to converge faster with k-point grid than the electronic contributions. This is largely due to a double cancellation of errors when we calculate $\varepsilon_{Relax}(\text{k-grid})$ from values of ε_{form} which already contain a cancellation of errors. Hence, although we should use a 4x4x4 grid to obtain an accurate value for $\varepsilon^{Relaxed}_{form}$, we find that much calculation time can be saved by estimating ε^{Rel}_{form} as

$$\begin{aligned} \varepsilon^{Rel}_{form} &\approx \varepsilon^{Unrel}_{form}(\text{4x4x4}) - \varepsilon_{Relax}(\text{2x2x2}) \\ &= \varepsilon^{Rel}_{form}(\text{2x2x2}) - \varepsilon^{Unrel}_{form}(\text{2x2x2}) + \varepsilon^{Unrel}_{form}(\text{4x4x4}) \end{aligned} \tag{3}$$

The resulting values of ε^{Rel}_{form} are converged to about $O(0.02\mathrm{eV})$.

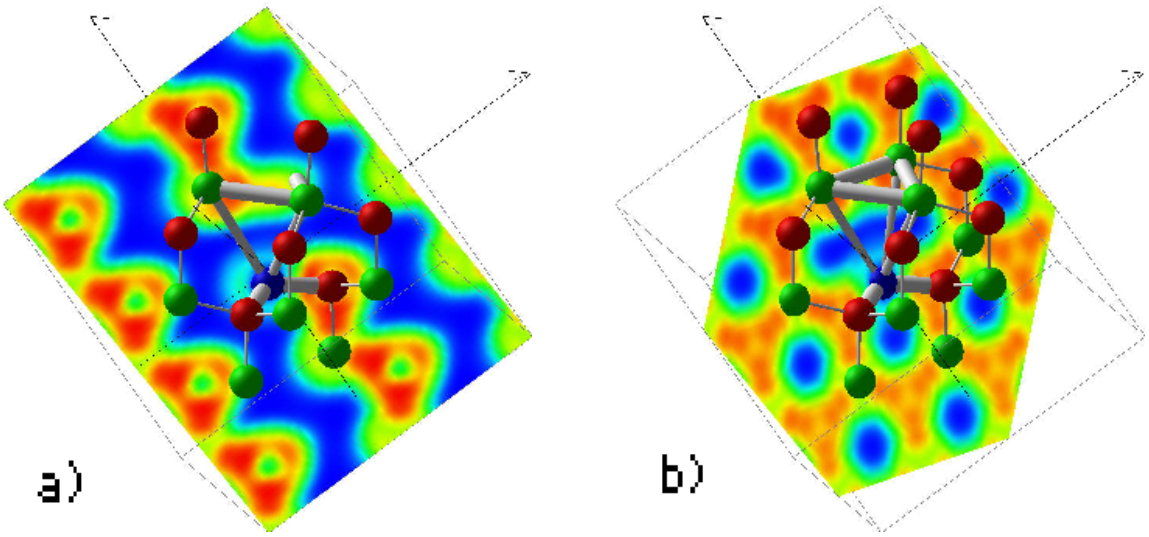

Figure 2. a) ELF plots for the $\left[Zn_{In}\text{-}V_P\right]^0$ complex. For clarity most atoms are omitted, and lines have been added between the Zn and the three In. In fact there are *no* Zn-In bonds. a) ELF in plane containing (111) b) ELF in plane containing Zn and 2 In.

Table 2. Transfer levels of $Zn_{In}\text{-}V_P$ in the 64 atom cell.

Level	Energy
+2/+1	-0.13 eV
+1/0	-0.26 eV
0/-1	0.59 eV
-1/-2	0.75 eV
-2/-3	0.96 eV

Table 3. Geometry of $\left[Zn_{In}\text{-}V_P\right]^Q$ as a function of Q.

Q	Zn-P	Zn-In	In-In	Volume
+1	2.30 Å	4.70 Å	4.37 Å	10.93 Å^3
+0	2.30 Å	4.41 Å	3.68 Å	7.55 Å^3
-1	2.30 Å	4.28 Å	3.47 Å	6.57 Å^3
-2	2.31 Å	4.17 Å	3.30 Å	5.84 Å^3
-3	2.31 Å	4.09 Å	3.17 Å	5.32 Å^3

3. Structure of the $Q = 0$ charge state.

In figure 1 we show the relaxed structure of the $Zn_{In}\text{-}V_P$ complex in the $Q = 0$ charge state, in the 64 atom supercell. The Zn_{In} is bonded to three P atoms only, and has relaxed back into a DX-like position in the same plane as them. The resulting Zn-P distances are 2.31 Å, which is almost identical to the Zn-P distance we find in a similar DFT-LDA calculation for ZnP_2 and various other Zn-P binary compounds. [3] The three In atoms on the other side of the V_P have moved together slightly, giving In-In distances of 3.68 Å, compared to an ideal

LDA bulk next nearest neighbout distance of 4.12 Å. The Zn-In distance is longer than the bulk value, however, at 4.41 Å. This gives a volume for the vacancy of 7.55 Å^3, where we calculate simply the volume of the tetradehron formed by the three In and the Zn. (NB: in all further figures most of the atoms in the cell are omitted for clarity, and fictitious bond lines are drawn between the Zn and the three In to guide the eye.) Examining the Electron Localisation Function (ELF) plots in figure 2 it can be seen that there is no bonding between Zn and the In triangle. Instead the Zn has three sp^2 hybrid orbitals bonded to the surrounding P, these bonds being filled. There is no charge density or ELF density related to the Zn along the line perpendicular to the Zn-P plane. This indicates that the single Zn p^z orbital left over from the formation of the sp^2 hybrids is empty.

4. Structure of the $Q \neq 0$ charge state.

In table 2 we give the positions of the first few transfer levels of the complex, as calculated in the 64 atoms cell. The structure of all of the states we have examined (+2 $\rightarrow$ -3) are very similar. (See table 3.) The Zn always lies in a DX-like position, with 2.31 Ålongsp^2 hybridised bonds to the three surrounding P atoms. The three In atoms always remain unbonded to Zn, but both the In-In distances and the Zn-In distances shorten with increasing negative charge. This then reduces the vacancy volume at each step, as listed in table 3.

In figure 3 we show the instantaneous change in charge density when an electron is added to (top row) or removed from (lower row) the $Q = 0$ charge state. IE: we take the $Q = 0$ relaxed positions, and calculate with the $Q = -1$ or $Q = +1$ total charge. We then subtract from this new charge density the original charge density from the relaxed $Q = 0$ calculation. The isocharge surfaces plotted are for 80%, 50% and 20% of the peak value. It is clear that an electron added goes to a localised orbital on or near the In triangle. An electron removed, however, comes from a delocalised state. We note, however, that even for the 20% peak value isocharge surfaces, the total charge enclosed corresponds to only 0.26 and 0.48 electrons respectively. Even for the $Q = -1$ charge state most of the added electron has an apparently delocalised character. This is, however, a results of the use of a relatively small supercell: the In-In distance is 3.7 Å *within* the cell, but about 8 Å in the opposite direction. This produces a significant false dispersion for the defect levels, and means that the transfer levels given in table 2 certainly should not be trusted.

In figure 4 we show the 50% peak isocharge surface for the instantaneous charge density change upon adding or removing electrons from the $Q = +1$, $Q = 0$, $Q = -1$, and $Q = -1$ relaxed geometries. The orbital filled when adding an electron to $Q = 0$ and that emptied when removing an electron from $Q = -1$ are rather similar. Clearly $Q = -1$ is a localised state of the Zn_{In}-V_P complex. The $Q = -2$ state is the same and indeed seems to have a very similar shaped orbital - probably the opposite spin state of the same orbital. That filled when adding a further electron to the relaxed $Q = -2$ has a different shape, but it too seems to be localised chiefly upon the In triangle.

Removing an electron from $Q = 0$ emptied a delocalised valence band state. However, adding an electron to the (fully relaxed) $Q = +1$ fills an In triangle localised orbital, none the less. Clearly $Q = +1$ also corresponds to a localised state of the complex, but more structural relaxation was needed in order to stabalise the localised state. Once stabalised, however, a further electron removed ($Q = +1 \rightarrow Q = +2$) seems to come from the same orbital again.

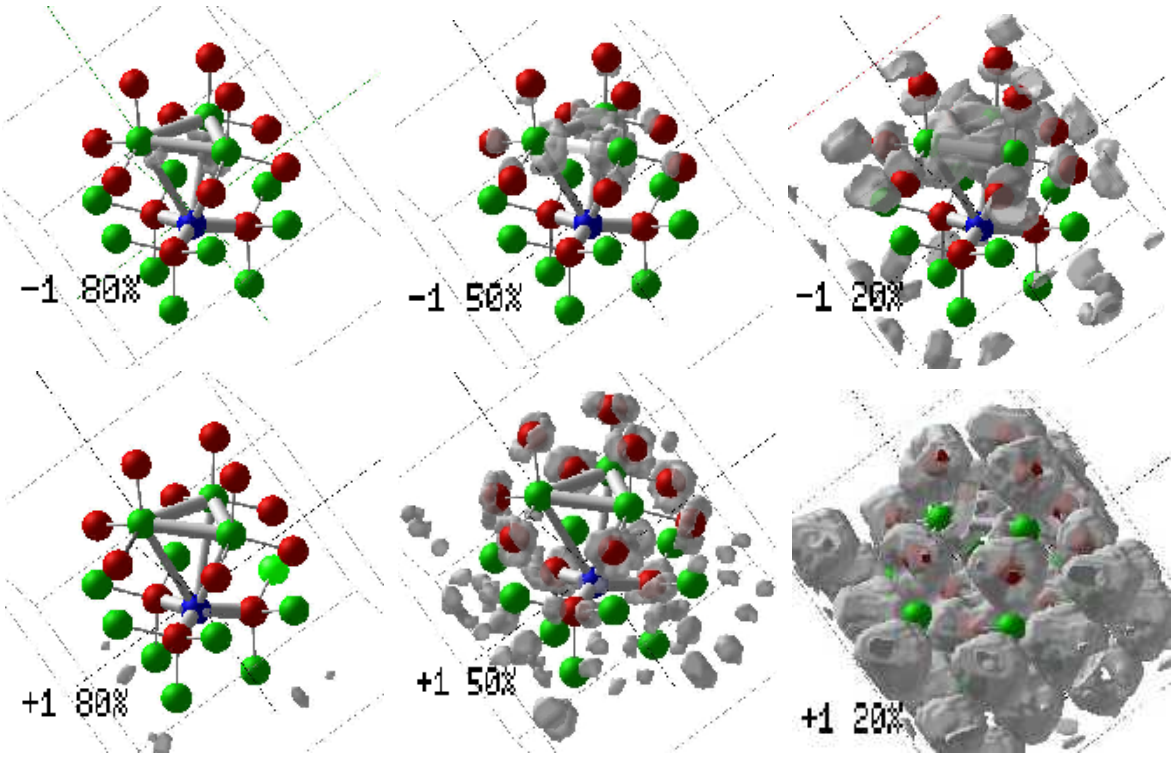

Figure 3. Charge density difference plots for the Zn_{In}-V_P complex in the $Q = 0$ relaxed geometry, but with an extra electron added (top row) or removed (lower row). Shown are isocharge surfaces for the charge density difference itself. The isocharges shown are for 80%, 50% and 20% of the peak value.

5. Conclusions.

To summaries, the Zn_{In}-V_P complex seems to have various stable charge states, differing by the addition or removal of electrons from localised orbitals centred on the In triangle. No electrons added or removed ever go on or near the Zn atom. It remains always in a DX like position, sp^2 hybridised, with an empty p^z orbital directed towards the In triangle, and very constant bond lengths to the surrounding P atoms.

On the other hand, we have shown that In-In distances, Zn-In distances and the vacancy volume of the complex are always reduced with increasing negative charge. The reduction in In-In distances is due simply to increased bonding, but the reduction in Zn-In distances is apparently electrostatic in origin. The empty Zn p^z orbital leave the positive ion core slightly less well screened along the direction pointing towards the three In atoms, in all charge states. Meanwhile the negative charge on the In atoms increases with the number of localised electrons on the complex, so the Zn-In distance is reduced electrostatically. The combination of the increased In-In bonding and increased Zn-In electrostatic attraction is then responsible for the reduction in effective vacancy volume within the complex. This structural model for the Zn-V_P complex, identified here as Zn_{In}-V_P , seems to be in good agreement with the experimental results of Slotte et al. [2], which showed reduced volume upon excitation of Zn_{In}-V_P . Our 0/-1 transfer levels is a little high for this, but, as was noted, these transfer levels are not reliable since the supercell is too small. Further studies of the complex in larger cells are required to check how this effects the position of the transfer levels.

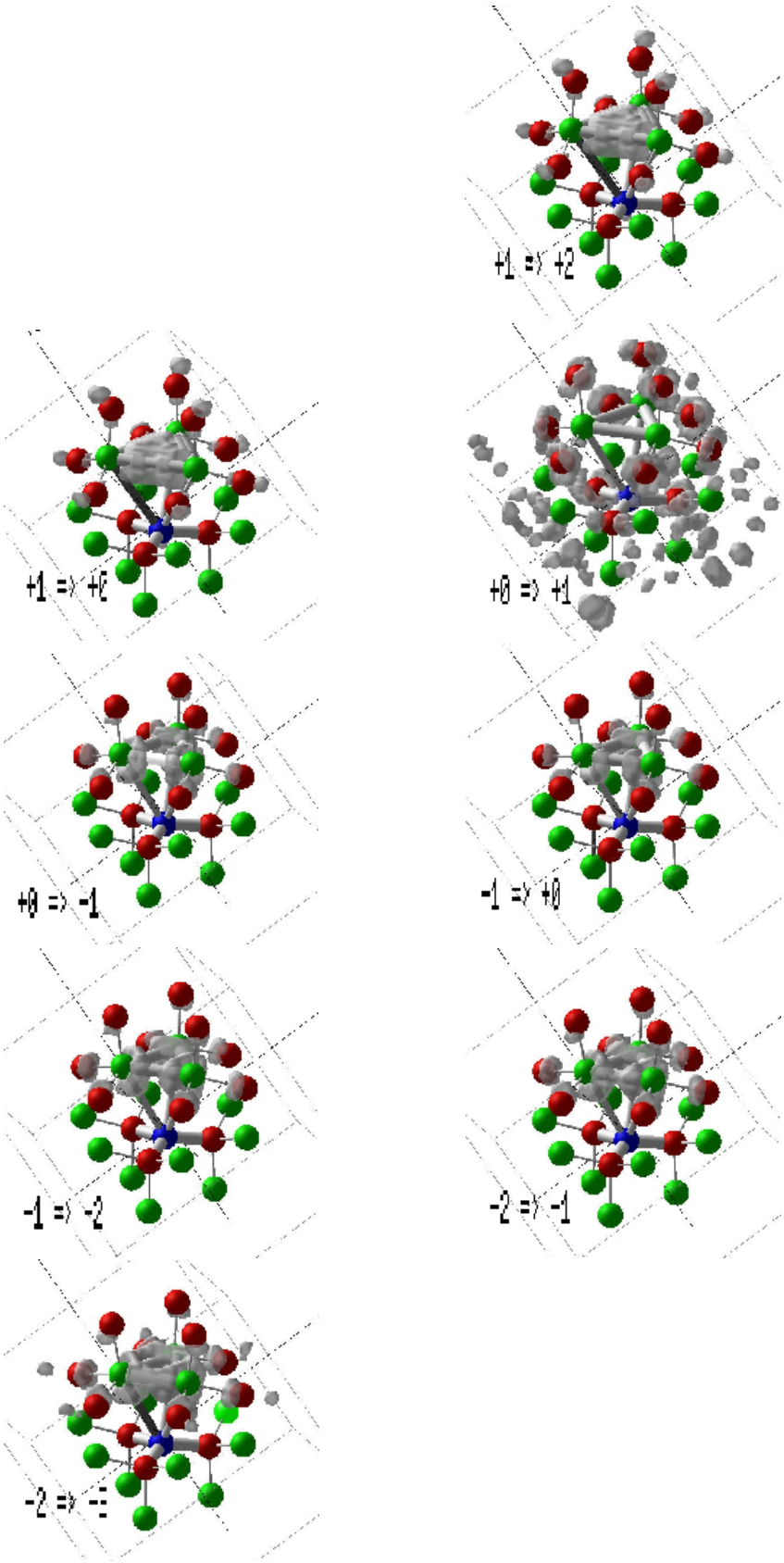

Figure 4. $\left[Zn_{In}\text{-}V_P\right]^Q$ 50% isocharge difference plots. The left collumn is for adding electrons to relaxed geometries of Q = +1, 0, -1 and -2 (downwards). The right collumn is for for removing electrons from relaxed geometries of Q = +1, 0, -1 and -2 (downwards).

References

[1] Mahony J, Mascher P, Puff W 1996 J. Appl. Phys. 80, 2712-2719
[2] Slotte J, Saarinen K, Salmi A, Simula S and Hautoj/”arvi P 2002 Preprint.
[3] Castleton C.W.M. Unpublished.